31st International Conference Nuclear Energy for New Europe
NENE 2022 September 12-15 PORTOROŽ SLOVENIA

Dynamic Mode Decomposition Analysis of a Cooling Channel of the TRIGA Mark II Reactor

Carolina Introini, Vittoria Brega, Antonio Cammi
Politecnico di Milano, Department of Energy
via La Masa 34
I-20156, Milan, Italy
carolina.introini@polimi.it; vittoria.brega@mailpolimi.it; antonio.cammi@polimi.it

ABSTRACT

As nuclear reactors present unique features compared to conventional systems, identifying the best-performing advanced modelling strategies remains an ongoing challenge from the point of view of accuracy and efficiency, especially for the safety aspect. In this context, Model Order Reduction (MOR) techniques offer a promising solution to the trade-off between solution accuracy and computational times, especially for multi-query scenarios. Traditional MOR techniques have been successfully applied in the nuclear engineering community to study the long-term behaviour of the system, however model-based MOR presents the computational bottleneck of needing evaluations of the full-order system in order to provide the data to build the reduced model.

Dynamic Mode Decomposition (DMD) is an equation-free MOR technique able to represent even complex models with explicit temporal dynamics based only on the observed data, without requiring any knowledge of the underlying governing equations. DMD allows the extraction of the time-varying characteristics of the system and of the governing dynamic structures from the available snapshots and, compared to other MOR methodologies, allows the evaluation of a low-dimensional surrogate of the dynamic matrix **A**, on which dynamic and stability analysis can be performed, and to predict the future system behaviour even without observations. As its application for nuclear-related applications is still not widespread, this work carries out an optimisation of the DMD algorithm for the reconstruction and prediction of reactor transients. The selected benchmark test case is a cooling channel of the TRIGA Mark II Reactor, with the aim of optimising the algorithm for its future application on the whole reactor system. The results show how providing enough data available at the beginning of the transient, DMD is able to correctly predict the pseudo-steady-state behaviour of the system even in absence of data.

1 INTRODUCTION

With the shift of reactor modelling towards large-scale, time-dependent analysis, the primary industry challenge is now the optimisation of the numerical simulations, computational algorithms and physical experiments. The aim is to reduce the economic cost of simulating such complex and large geometries while at the same time satisfying the ever-increasing safety requirements. Despite the advancements in computational resources, large-scale modelling is still

not feasible for all those applications that require real-time analysis, such as dynamic monitoring and control, which should be accurate but at the same time fast enough to identify potentially critical situations ahead of time; they require fast and reliable methods to identify the evolving dynamics of the system [1]. In this sense, the MOR framework represents a potential solution to develop sufficiently accurate but fast models.

In particular, non-intrusive data-driven MOR (DA-MOR) aim to generate low-fidelity models and to extract the dominant patterns exhibited by transient processes starting from some high-fidelity snapshots or experimental data, therefore without the need for additional approximations of the physics of the system. Among all DA-MOR methods, Dynamic Mode Decomposition (DMD) is of particular interest mainly because of its ability to represent even complex models with explicit temporal dynamics based only on observed data [2]. In addition, DMD produces a low-dimensional surrogate of the dynamic matrix $\mathbf{A}$, whose eigenvalues are equal to those of the unknown full-dimensional matrix: as such, it is possible to set up an eigenvalue problem to study the asymptotic behaviour of the full order system. DMD is based on the singular value decomposition (SVD) and Koopman theory [3] to reduce the dimension of the system under analysis by extracting spatially correlated structures with the same linear behaviour in time. Being based purely on measurement data, DMD does not require any knowledge of the governing equations [4]. Several applications of the DMD algorithm can be found in literature, especially in the Computational Fluid Dynamics field [4]. However, the use of DMD in the nuclear reactor field is still scarce: following the work done in [5], this work extends the application to a three-dimensional cooling channel of the TRIGA Mark II reactor of the University of Pavia, to provide a preliminary benchmark for the analysis of the full reactor [6].

Section 2 presents the formulation of the DMD algorithm adopted in this work. Section 3 discusses the results obtained by applying the DMD algorithm to a cooling channel of the TRIGA Mark II reactor at the University of Pavia.

2 DYNAMIC MODE DECOMPOSITION

DMD techniques seek the linear dynamic operator that best approximates the underlying dynamics of the system and, because of its theoretical foundation, the DMD algorithm can also describe the non-linear dynamics [7]. Based on the use of either empirical or simulated snapshots, DMD seeks an eigenvalue-eigenvector decomposition in which the spatial modes (the eigenvectors) are built based on their dynamics properties and thus are associated with a dynamic spectrum (the eigenvalues). Thus, DMD aims at obtaining a finite-dimensional approximation by identifying an appropriate subspace spanned by a subset of the eigenfunctions of the operator itself. The advantages of this approach are several: for instance, DMD can extract any dynamically relevant structure, regardless of its energy. DMD also allows an equation-free modelling framework since it does not require any projection of the modes to get time-dependent coefficients.

2.1 The DMD Algorithm

When considering a time series of data at a grid of spatial locations, the first step is to flatten the three-dimensional fields of interest at time t_k into a single tall column vector, a snapshot of data. This step removes the spatial relationship between neighbour cells, still allowing the comparison of these snapshots using inner vector products. The size n of the snapshots depends on the numerical grid and the number of variables of interest. When sorted, these snapshots represent the evolution in time of the state of the system, and they are collected

in pairs denoted by $\{x(t_k), x(t'_k)\}_k^M$, where $t'_k = t_k + \Delta t$ under the assumption that the selected time-step Δt is sufficiently small to resolve the highest frequencies in the dynamics. These snapshots are arranged into two data matrices:

$$\mathbf{X} = [\mathbf{x}(t_1), \mathbf{x}(t_2), ..., \mathbf{x}(t_m)] \qquad \mathbf{X}' = [\mathbf{x}(t'_1), \mathbf{x}(t'_2), ..., \mathbf{x}(t'_m)] \tag{1}$$

Usually, the size n of these data matrices is much larger than the number of available snapshots m, differently from literature where a collection of measurements in time are typically row vectors. The DMD procedure operates the spectral decomposition of the best-fit linear operator $\mathbf{A}$ that relates the two snapshots matrices in time, that is, the operator that establishes a linear dynamical system that best advances snapshots forward in time:

$$\mathbf{X}' \approx \mathbf{A}\mathbf{X} \tag{2}$$

Mathematically, the best-fit operator $\mathbf{A}$ is defined as:

$$\mathbf{A} = argmin_{\mathbf{A}} ||\mathbf{X}' - \mathbf{A}\mathbf{X}||_F = \mathbf{X}'\mathbf{X}^\dagger \tag{3}$$

where $||\cdot||_F$ is the Frobenius norm and $\dagger$ denotes the pseudo-inverse. For a high-dimensional state vector $\mathbf{x} \in \mathbb{R}^n$, the matrix $\mathbf{A}$ has n^2 elements, and for all but small and simple system its spectral decomposition is not computationally achievable. Through reduction, the DMD algorithm extracts the dominant eigenvalues and eigenvectors of $\mathbf{A}$ by computing the pseudo-inverse $\mathbf{X}^\dagger$ using the singular value decomposition of the matrix $\mathbf{X}$. Typically, this matrix has fewer columns m than rows n, meaning that there are at most m non-zero singular values (and respective singular vectors) and that the matrix $\mathbf{A}$ will have at most rank m. By projecting $\mathbf{A}$ onto these singular vectors, it can be approximated with a low-dimensional matrix $\tilde{\mathbf{A}}$ of size at most $m \times m$. Indeed, DMD aims at approximating the high-dimensional eigenvectors of $\mathbf{A}$ from its reduced approximation $\tilde{\mathbf{A}}$ and the data matrix $\mathbf{X}$ without computing the high-dimensional linear operator, and under certain conditions, these approximate modes are the exact eigenvectors of $\mathbf{A}$.

The rank of the data matrix $\mathbf{X}$ is at most m, so there are at most m non-zero singular values. Decomposition of the data matrix is performed through the SVD, using the method of snapshots to compute the leading terms in the SVD. The first step is to construct an $m \times m$ column-wise correlation matrix consisting of inner products of the columns of $\mathbf{X}$, whose eigendecomposition is related to the SVD:

$$\mathbf{X}^*\mathbf{X} = \mathbf{V}\mathbf{\Sigma}\mathbf{U}^*\mathbf{U}\mathbf{\Sigma}\mathbf{V}^* = \mathbf{V}\mathbf{\Sigma}^2\mathbf{V}^* \qquad \mathbf{X}^*\mathbf{X}\mathbf{V} = \mathbf{V}\mathbf{\Sigma}^2 \tag{4}$$

After computing $\mathbf{V}$ and $\mathbf{\Sigma}$ from the spectral decomposition of $\mathbf{X}$, the column of $\mathbf{U}$, which represent the spatial modes, are constructed:

$$\mathbf{U} = \mathbf{X}\mathbf{V}\mathbf{\Sigma}^{-1} \tag{5}$$

The space and time correlations are now separated into the matrices $\mathbf{U}$ and $\mathbf{V}$, respectively, whereas $\mathbf{\Sigma}$ contains the singular values of the data matrix. Projection methods disregard the time information contained in $\mathbf{V}$, whereas DMD uses the time correlation to rearrange the leading column of $\mathbf{U}$ to extract the dominant patterns in the subspace that remain coherent both in space and time. The SVD matrices have the following dimensions: $\tilde{\mathbf{U}} \in \mathbb{C}^{n \times r}$, $\tilde{\mathbf{\Sigma}} \in \mathbb{C}^{r \times r}$ and $\tilde{\mathbf{V}} \in \mathbb{C}^{m \times r}$, where $r \leq m$ denotes the rank of the data matrix $\mathbf{X}$. Choosing the reduction rank r is a critical step for all MOR techniques. Many factors, such as the dimension of the

reduced space and the magnitude of noise, influence the choice of r. A straightforward procedure is to select r such that the estimated truncation error reaches a threshold value: singular values that fall below this threshold are deemed not to contain important information and thus discarded. From this, the low-dimensional surrogate $\tilde{\mathbf{A}}$, along with its spectral decomposition, can be computed:

$$\tilde{\mathbf{A}} = \tilde{\mathbf{U}}^* \mathbf{X}' \tilde{\mathbf{V}} \tilde{\mathbf{\Sigma}}^{-1} \qquad \tilde{\mathbf{A}}\mathbf{W} = \mathbf{W}\mathbf{\Lambda} \tag{6}$$

The essential passage in the DMD procedure is that the reduced matrix $\tilde{\mathbf{A}}$ has the same non-zero eigenvalues as the full matrix $\mathbf{A}$. Therefore, there is no need to compute the high-dimensional matrix since its reduced approximation is sufficient to extract the leading r eigenvalues. The matrix $\tilde{\mathbf{U}}$ containing the modes represents the map to reconstruct the full-order state x from the reduced one, whose linear evolution in time can be written as:

$$\tilde{\mathbf{x}}_{k+1} = \tilde{\mathbf{A}}\tilde{\mathbf{x}}_k \tag{7}$$

The entries of the diagonal matrix $\mathbf{\Lambda} \in \mathbb{R}^{r \times r}$ are the DMD eigenvalues, equal to the ones of the full order matrix. The columns of $\mathbf{W} \in \mathbb{R}^{r \times r}$ are the eigenvectors of $\tilde{\mathbf{A}}$ and they represent a linear combination of POD modes amplitudes that behave linearly with the temporal pattern given by λ. The high-dimensional DMD modes $\mathbf{\Psi}$ can be reconstructed using the eigenvectors $\mathbf{W}$ and the time-shifted measurements matrix, and they correspond to the first r eigenvectors of the full order matrix $\mathbf{A}$:

$$\mathbf{\Psi} = \mathbf{X}' \tilde{\mathbf{V}} \tilde{\mathbf{\Sigma}}^{-1} \mathbf{W} \tag{8}$$

To find a DMD mode corresponding to $\lambda = 0$, the projected mode $\psi = \tilde{\mathbf{U}}\mathbf{w}$ should be used. Through DMD, the system state can be expanded in terms of a data-driven spectral decomposition (either by using the discrete or the continuous-time eigenvalues, respectively λ or ω):

$$\mathbf{x}_k = \mathbf{\Psi}\mathbf{\Lambda}\mathbf{b} = \mathbf{\Psi}\exp(\mathbf{\Omega}t)\mathbf{b} = \mathbf{\Psi}\exp(\mathbf{\Omega}t)(\mathbf{W}\mathbf{\Lambda})^{-1}\tilde{\mathbf{x}}_1 \qquad \omega = \frac{\log \lambda}{\Delta t} \tag{9}$$

where b_j is the mode amplitude.

3 TEST CASE

As a preliminary test case, this work considers a CFD model of an instrumented cooling channel of the reactor core, using the open-source code OpenFOAM [8] to retrieve the FO snapshots. The considered channel has a total power of 25578 W and a Reynolds number close to the fully turbulent regime. The main geometric parameters of the channel and mesh characteristics are summarised in Table 1. The grid presents coarse axial refinement to reduce the computational cost of the FO simulation, and the optimal number of axial divisions is the one found in the analysis performed in [9]. The grid presents small layers near the walls to allow the accurate resolution of turbulence.

The inlet velocity is taken as an input parameter from the full core simulation performed in [10]. For temperature, the model uses as an inlet value a time-varying series according to the value of the lowermost experimental sensor, to simulate the heating of the whole reactor during the transient. Turbulent quantities (dissipation rate, kinetic energy, specific dissipation rate) at the inlet use free stream values. Finally, the model uses an outflow condition for the outlet boundary condition. More details on the CFD model, along with a grid independence study, can be found in [6]. The average sampling time used in the experimental campaign is equal to 15.6 seconds, for a total of 130 minutes (7800 seconds) and a total of 500 snapshots.

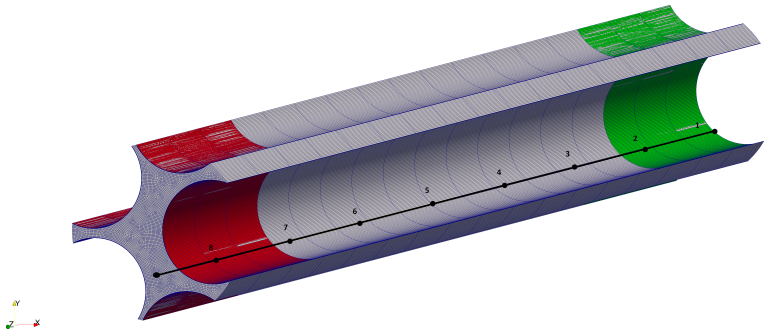

Figure 1: Geometry and numerical mesh of the adopted single channel (lateral view). The red and green regions indicate the upper and lower axial reflector, respectively. The black line represents the measurement rod within the channel, with the axial position of the sensors (from 1 to 8 bottom to top)

Table 1: Channel geometric parameters and main mesh characteristics

Parameter	**Symbol**	**Value**
Hydraulic diameter	d_H	0.023 m
Hydraulic area	A_H	0.000987 m^2
Wetted perimeter	P_w	0.177 m
Channel height	h	0.585 m
Active height	h_a	0.381 m
Elements		320943
Type		Hexaedral
Non-orthogonality		9.283
Max skewness		3.298
y^+		≈ 0.5

4 RESULTS

The two relevant parameters for the DMD analysis presented below are the truncation rank r and the index of the last snapshots taken for the reconstruction (k). This latter parameter indicates when the data acquisition for the full-order model is stopped: beyond this index, no full-order information is available, and the DMD rather than reconstruct the fields tries to predict them based on the extracted dynamics.

Following the computation of the full-order solution, the first step is to assess the reducibility of the system under consideration. As there is no *a-priori* information about the system, it is assumed that it decays fast with an increasing dimension of the reduced space. For *a-posteriori* verification of this behaviour, the first step is to plot the decay rate of the normalised singular values for temperature and velocity, ranked in decreasing order (Figure 2a). Their behaviour shows the strong reducibility of the considered test case, especially for temperature. Especially for temperature, with only 5 bases the sorted normalised eigenvalues drop below 10^{-9}. The exponential decay of the eigenvalues is less pronounced for velocity, but still few bases are enough to drop their value below 10^{-9}.

Further confirmation of the good reducibility of the problem is given by the normalised L^2 error, computed as:

$$e_{M,\mathcal{X}} = \frac{||u(\cdot,\mu) - \mathcal{P}_M[u(\cdot,\mu)]||_{L^2}}{||u(\cdot,\mu)||_{L^2}}, \tag{10}$$

where u is the field of interest (either velocity or temperature in this test case), $\mu \in \Xi_{test}$ and $\mathcal{P}$ is the projection operator. Figure 2b shows the maximum L^2 error for velocity and temperature. Following a fast decay below 10^{-3}, the decrease of the decay error slows dramatically, meaning that after a certain dimension of the reduced space additional bases are adding little information to the reduced-order model. In particular, eight bases are enough to drop the error below 10^{-3}, and this value has been taken as a truncation rank for the reconstruction.

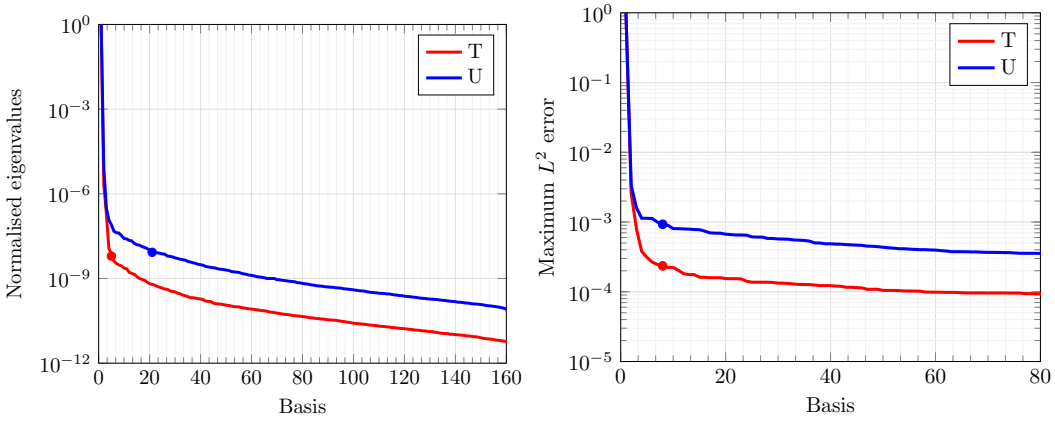

(a) scale=0.9 (b) scale=0.9

Figure 2: (a) Normalised eigenvalues for temperature (red) and velocity (blue). The two dots indicate the reference value of 10^{-9} for comparison purposes ; (b) Reconstruction error for temperature and velocity in L^2 norm up to rank 80. The two dots reflect the error using rank 8, which corresponds to the number of sensors in the channel and therefore is a baseline for the case with experimental data only.

Figure 3 shows the residual (computed as the difference between the reference CFD solution and the DMD reconstruction) in the bulk of the cooling channel. In this case, the DMD rank was taken as 8, and all snapshots were considered in the analysis ($k = 500$). The residual remains below 1 °C during the whole transient, showing how the DMD can correctly reconstruct the field of interest. Conversely, Figure 4 shows the absolute residual for the velocity magnitude in the bulk of the cooling channel, with the same parameters as Figure 3. The obtained results confirm the capability of the DMD algorithm to reconstruct the fields of interest, as the maximum residual for velocity in the channel bulk is equal to 1.5e-3.

Figure 5 shows the local temperature profile in the channel as predicted by DMD, with $r = 8$, $\Delta t = 180s$ and $k = 300$: the vertical dashed line indicates the point at which the data acquisition is stopped. Compared to the full-order results, very good agreement is reached by the DMD reconstruction especially for the four lower locations, with the maximum discrepancy being roughly 1 °C at the end of the transient. For the four topmost locations, the maximum discrepancy rises to 3 °C. Nevertheless, these results show how the DMD algorithm can correctly predict the pseudo-steady-state for temperature beyond the last snapshot used for computing the DMD model following the initial transient growth.

Figure 6 shows the local velocity profile in the channel as predicted by DMD, with $r = 8$, $\Delta t = 180s$ and $k = 300$: the vertical dashed line indicates the point at which the data acquisition is stopped. Compared with the CFD results, the DMD can very accurately predict the local behaviour of velocity in the considered channels, even beyond the last snapshot used for computing the DMD model. Clearly, beyond $k = 300$ the agreement is worse, but the DMD can still predict with reasonable accuracy the pseudo-steady state. These two last results are

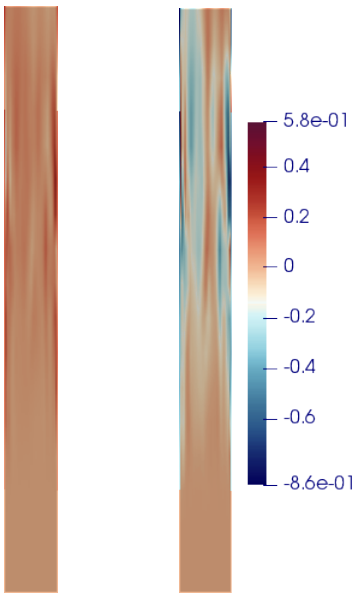

(a) 30 s (b) 130 s

Figure 3: Residual error computed as the difference between full-order and DMD reconstruction (with rank 8) for temperature in the channel bulk (mid-plane)

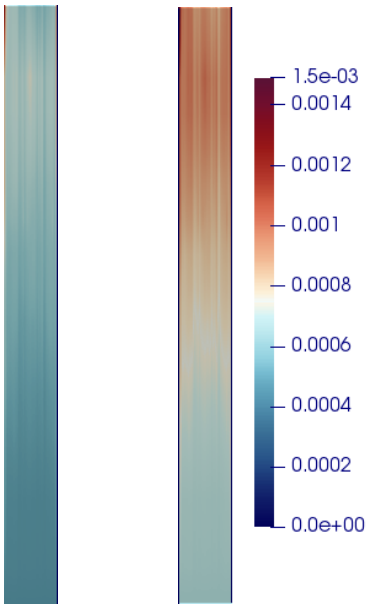

(a) 30 s (b) 130 s

Figure 4: Residual error computed as the difference between full-order and DMD reconstruction (with rank 8) for the velocity magnitude in the channel bulk (mid-plane)

especially relevant because it means that the accuracy in the DMD prediction is not limited to the average quantities, but it can be extended also to identify local, non-observed phenomena, thus proving the capability of DMD to extract the relevant dynamic information and to extend them beyond the available snapshots.

Table 2: Channel geometric parameters and main mesh characteristics

	DMD
Snapshots creation	4 CPU-hours
Offline phase	1 CPU-minute
Single online run	2 CPU-minutes
Read-write routines	6 CPU-hours

Table 2 reports the computational times required for the various step of the DMD method. Concerning the computational times for the DMD model, as expected the main bottleneck was found to be the conversion of the data from the OpenFOAM format to the MATLAB one (and vice versa), although this is a peculiarity of the implementation strategy chosen in this work. The former step is included in the offline phase and, once the data acquisition or the simulation has ended, it is performed only once. On the other hand, the singular value decomposition step, the evaluation of the DMD modes and the reconstruction (and prediction) are extremely fast, operating almost in real time.

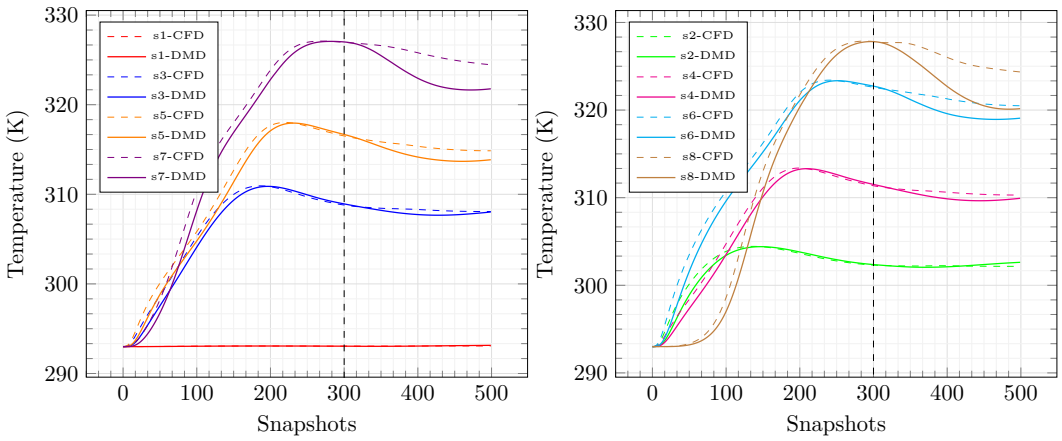

(a) Eigenvalues

(b) Error

Figure 5: Comparison of the temperature predicted by DMD with the CFD one, at a different height in the channels (each position is at 8 mm from the one below, from the bottom of the channel), with rank 8 and by stopping the data acquisition at the 300th snapshots out of 500.

5 CONCLUSIONS

This work shows the application of the DMD algorithm to a cooling channel of the TRIGA Mark II nuclear reactor at the University of Pavia. The proposed approaches were implemented in MATLAB, providing the main advantage of independence from the source of data. The algorithm was used to reconstruct the temperature and velocity fields. The results were very satisfactory, with the DMD algorithm able to correctly reconstruct the temperature and velocity fields with very good accuracy also in terms of local behaviour. In addition, good results were obtained in terms of state prediction, proving that DMD is indeed able to extract the dynamic structure of the system under analysis even without any knowledge about the mathematical model. As an accurate and fast algorithm in both the transient and steady-state reconstruction, DMD can also be used for control-oriented applications or real-time analysis.

REFERENCES

[1] J. F. Hauer, D. J. Trudnowski and J. G. DeSteese, “A perspective on WAMS analysis tools for tracking of oscillatory dynamics”, Proceedings of the IEEE/EPS General Meeting 2007, 2007.

[2] P. J. Schmidt, “Dynamic mode decomposition for numerical and experimental data”, Journal of Fluid Mechanics, 636, 2010, pp. 5-28.

[3] C. W. Rowley, I. Mezic, S. Bagheri, P. Schlatter, D. S. Henningson, “Spectral analysis of nonlinear flows”, Journal of Fluid Mechanics, 645, 2009, pp. 115-127.

[4] J. H. Tu, C. W. Rowley, D. M. Luchtenburg, S. L. Brunton, N. J. Kutz, “On dynamic mode decomposition: theory and applications”, Journal of Computational Dynamics, 1, 2014, pp. 391-421.

[5] A. Di Ronco, C. Introini, E. Cervi, S. Lorenzi, A. Cammi, “Dynamic Mode Decomposition for the Stability Analysis of the Molten Salt Fast Reactor Core”, Nuclear Engineering and Design, 362, 2020, no. 110529.

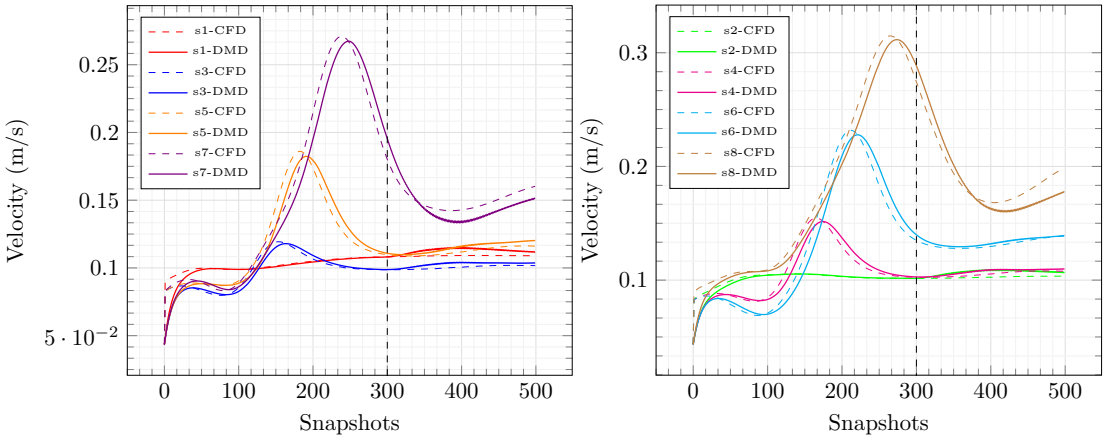

(a) Eigenvalues (b) Error

Figure 6: Comparison of the velocity magnitude predicted by DMD with the CFD one, at a different height in the channels (each position is at 8 mm from the one below, from the bottom of the channel), with rank 8 and by stopping the data acquisition at the 300th snapshots out of 500.

[6] C. Introini, "Advanced Modelling and Stability Analysis of Nuclear Reactors", PhD Thesis, Politecnico di Milano, 2021.

[7] N. J. Kutz, S. L. Brunton, B. W. Brunton, J. L. Proctor, "Dynamic Mode Decomposition: Data-Driven Modelling of Complex Systems", Society for Industrial and Applied Mathematics (SIAM), 2016.

[8] H. Weller, H. Jasak, C. Fureby. "A tensorial approach to computation continuum mechanics using object-oriented modelling", Computers in Physics, 12, 1998, pp. 620-631.

[9] C. Introini, S. Lorenzi, A. Cammi, "Comparison of several RANS modelling for the Pavia TRIGA Mark II research reactor", Proceedings of the International Conference Nuclear Energy for New Europe NENE, 2017, pp. 451-459.

[10] C. Introini, S. Lorenzi, A. Cammi, "A 3D CFD model for the study of natural circulation in the Pavia TRIGA Mark II research reactor", Proceedings of the International Conference Nuclear Energy for New Europe NENE, 2017, pp. 409-417.